Jets and High-p_T

Jets in p+p and A+A

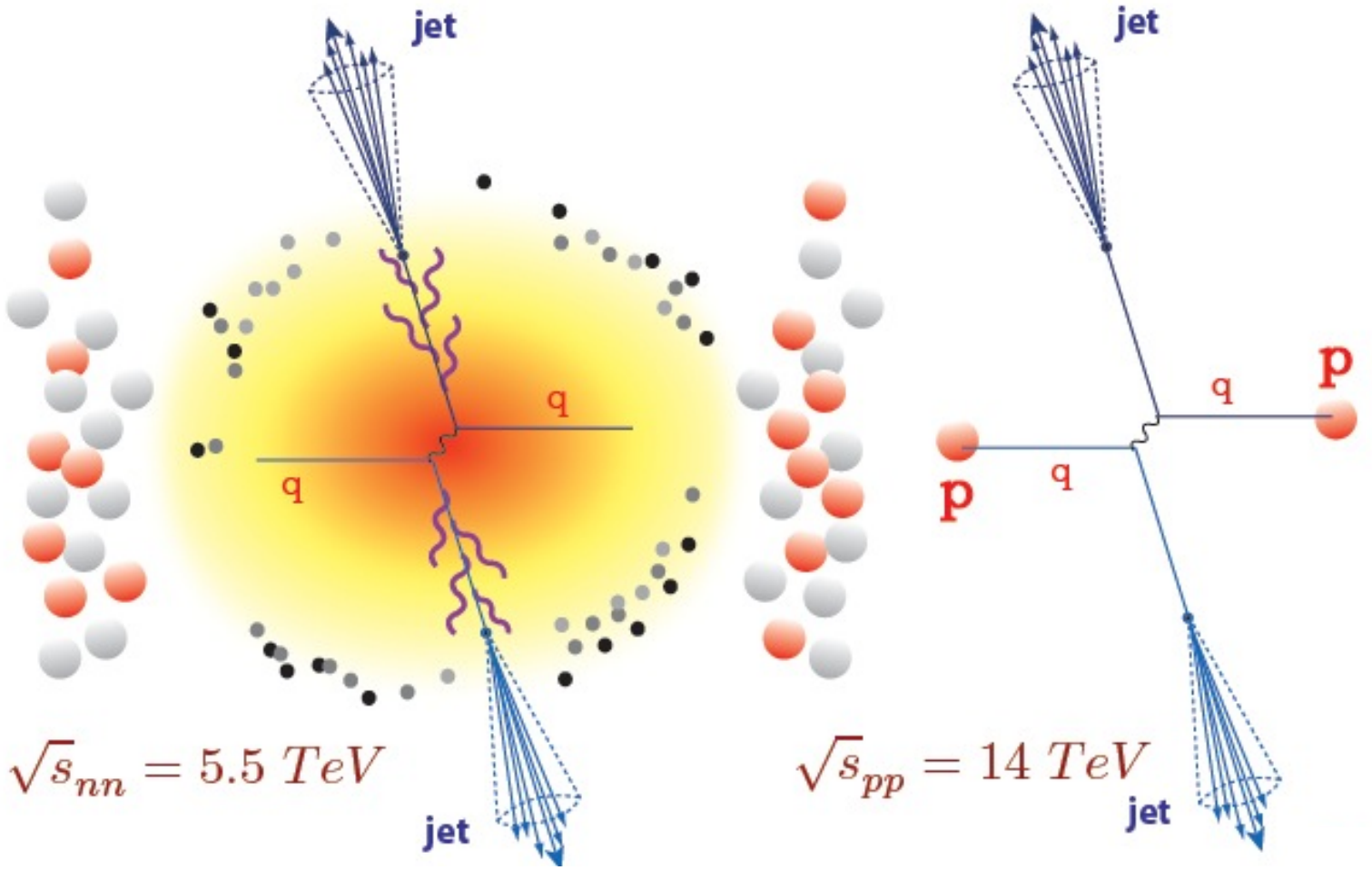

Jets in p+p

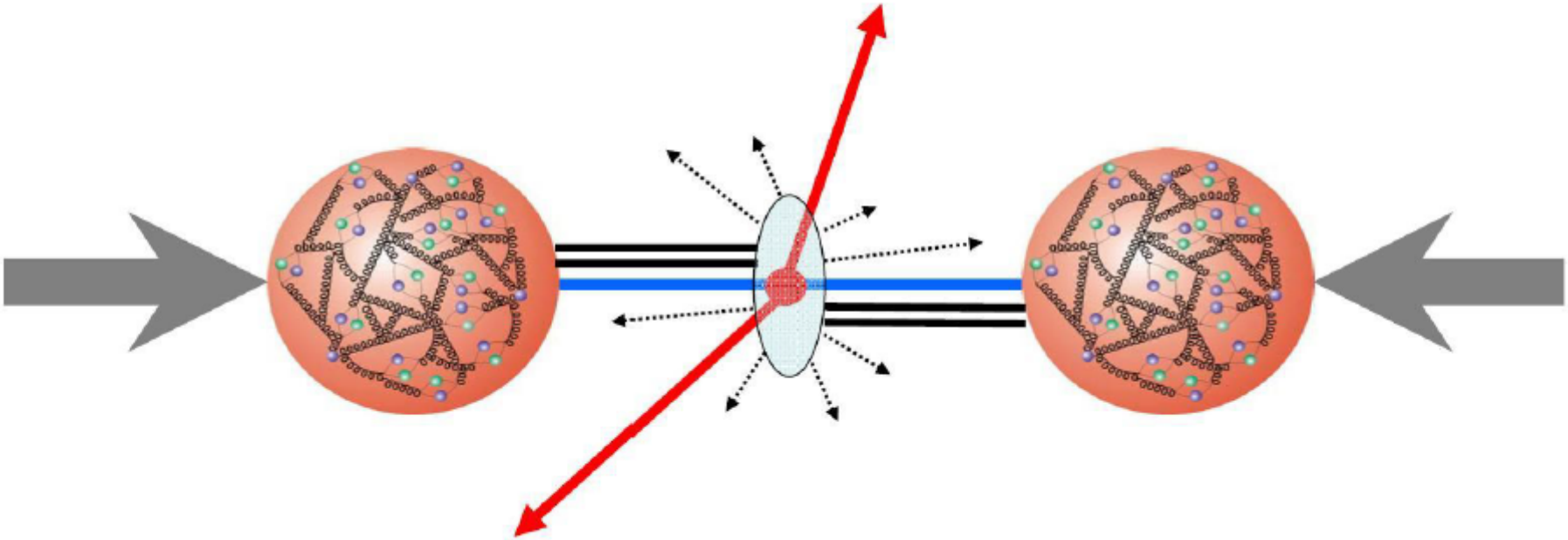

QCD Factorization

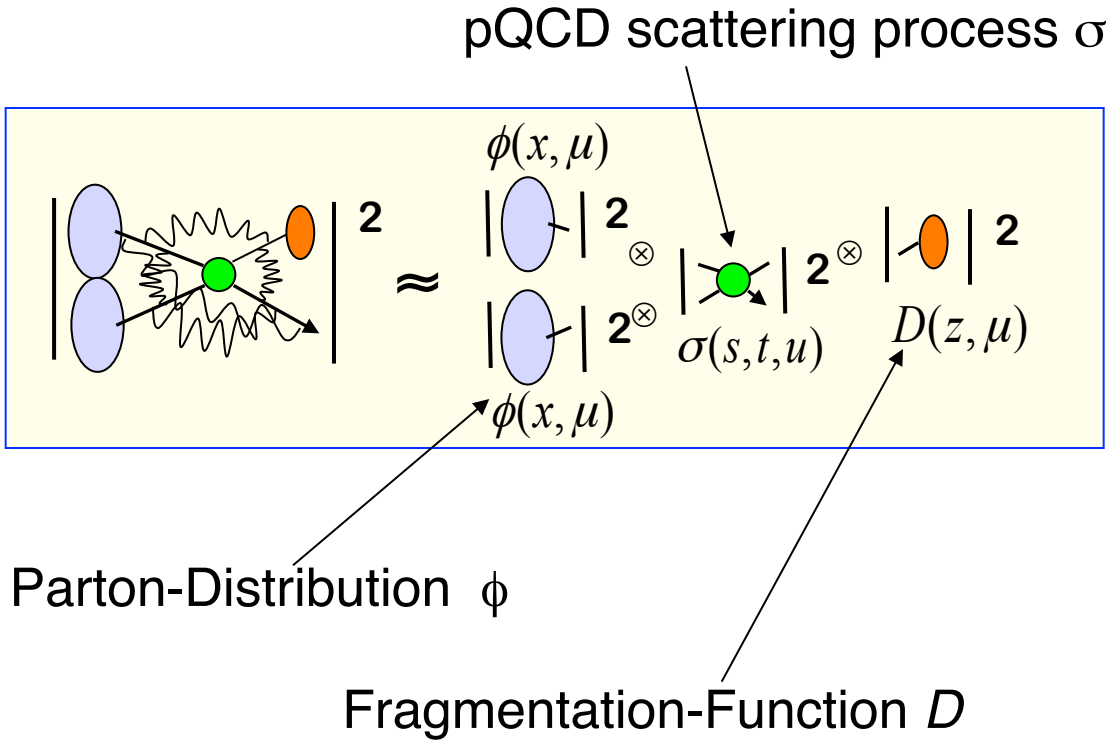

QCD Factorization

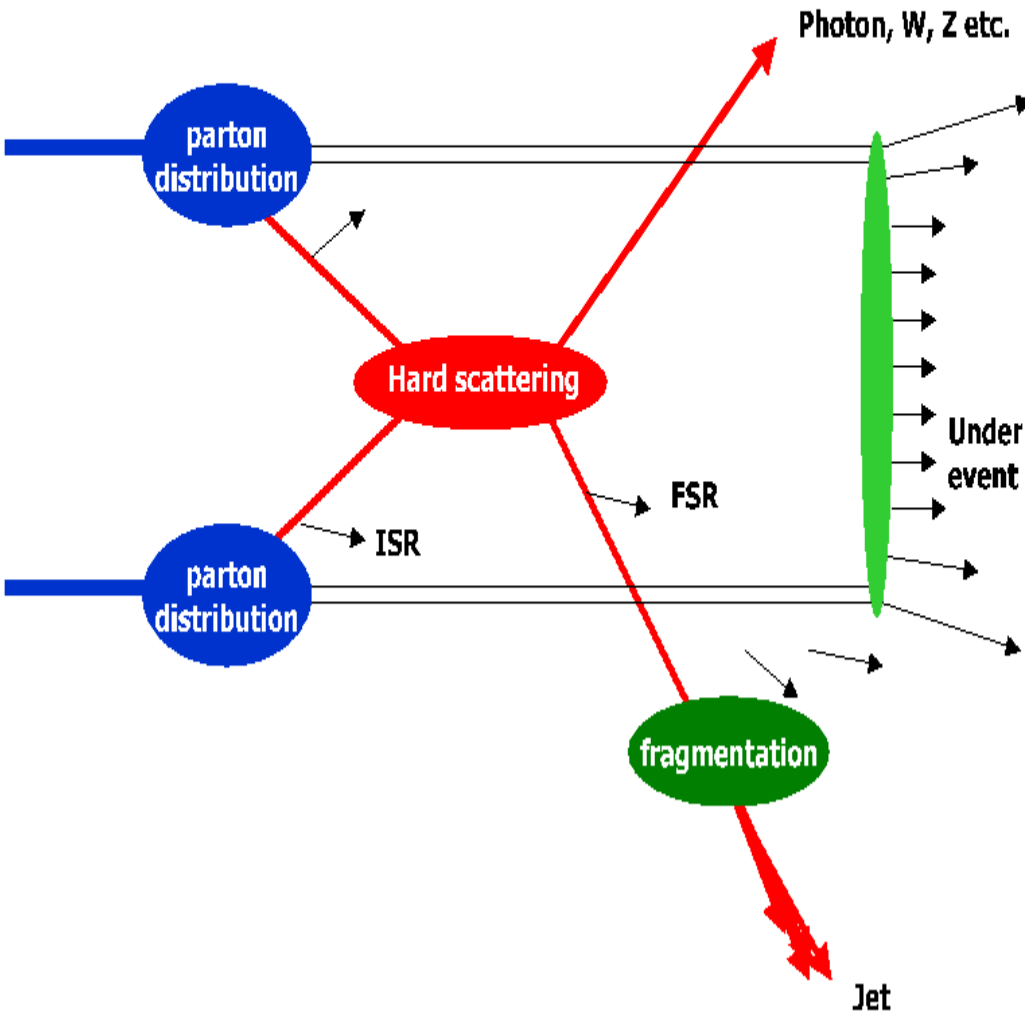

Structure function in a Parton-Modell

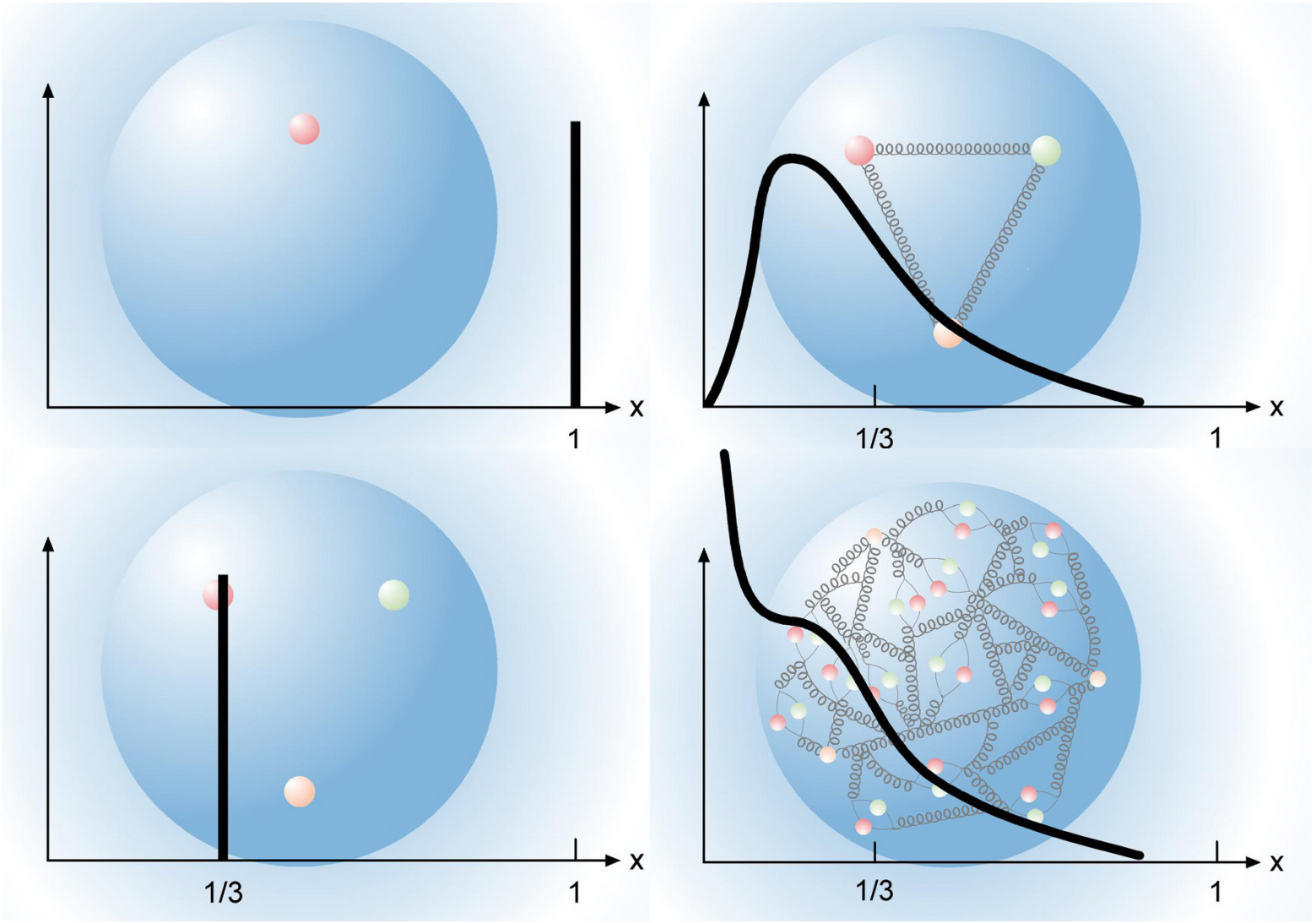

Parton distribution from deep inelastic scattering

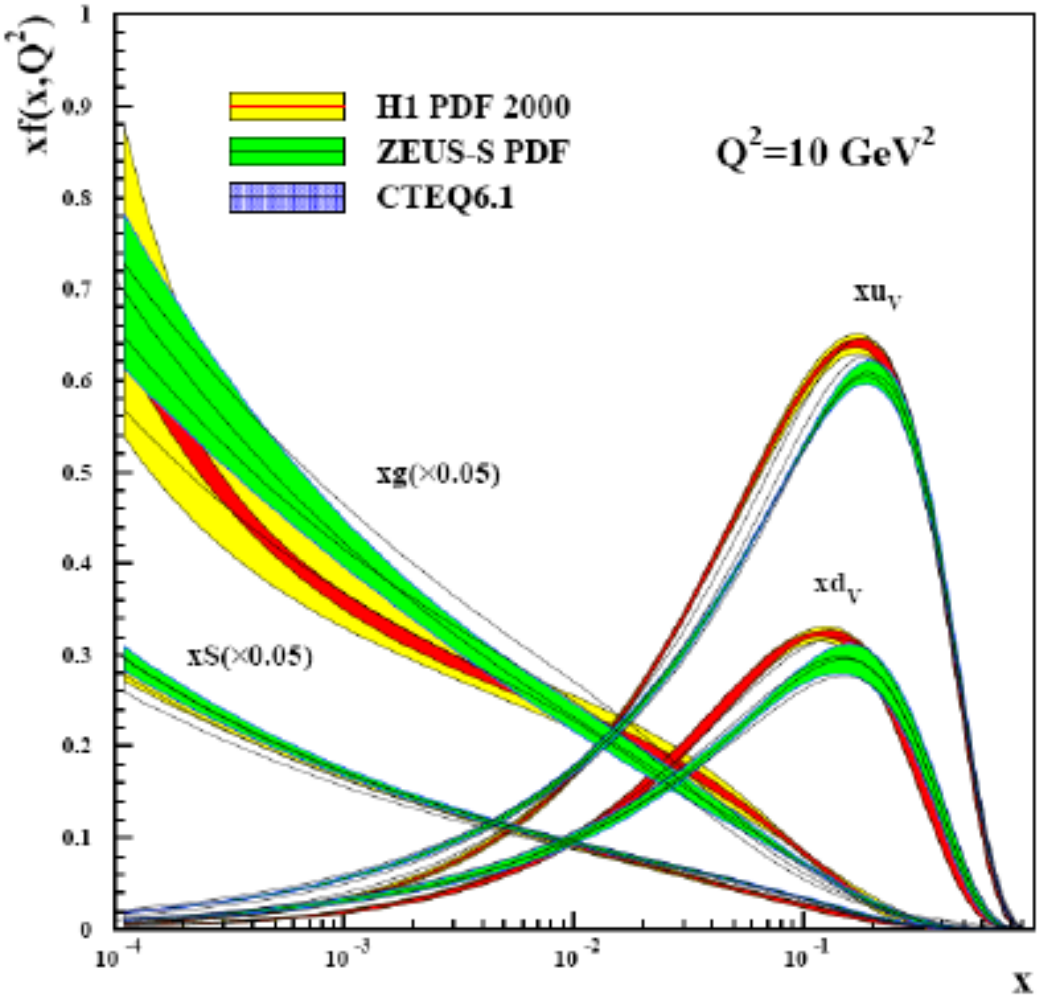

Fragmentation function

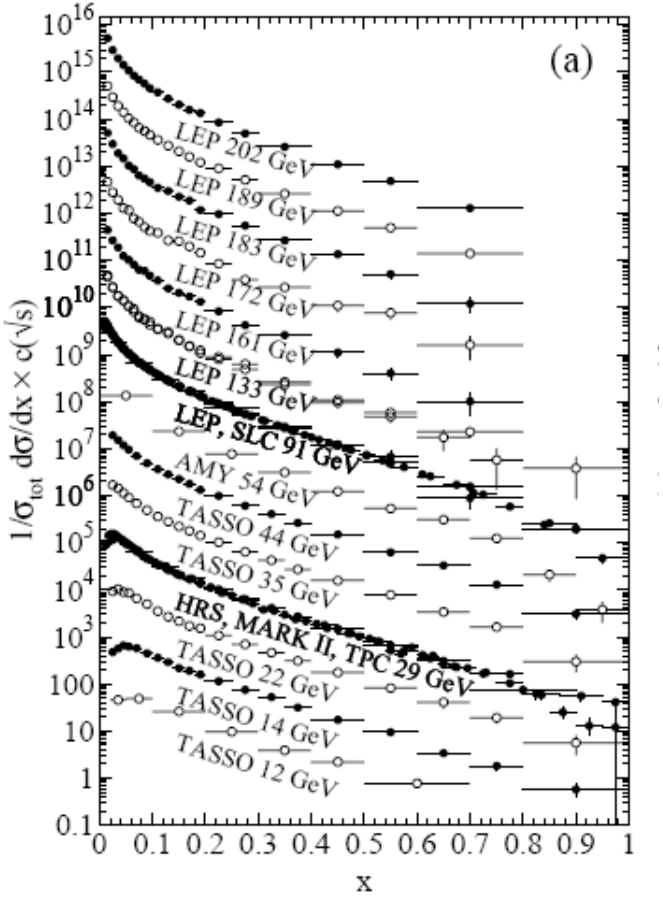

Figure 17.1: The e^+e^- fragmentation function for all charged particles is shown [9–25](a) for different c.m. energies, $\sqrt{s}$, versus x and (b) for various ranges of x versus $\sqrt{s}$. For the purpose of plotting (a), the distributions were scaled by $c(\sqrt{s}) = 10^i$ where i is ranging from $i = 0$ ($\sqrt{s} = 12$ GeV) to $i = 13$ ($\sqrt{s} = 202$ GeV).

Fragmentation function

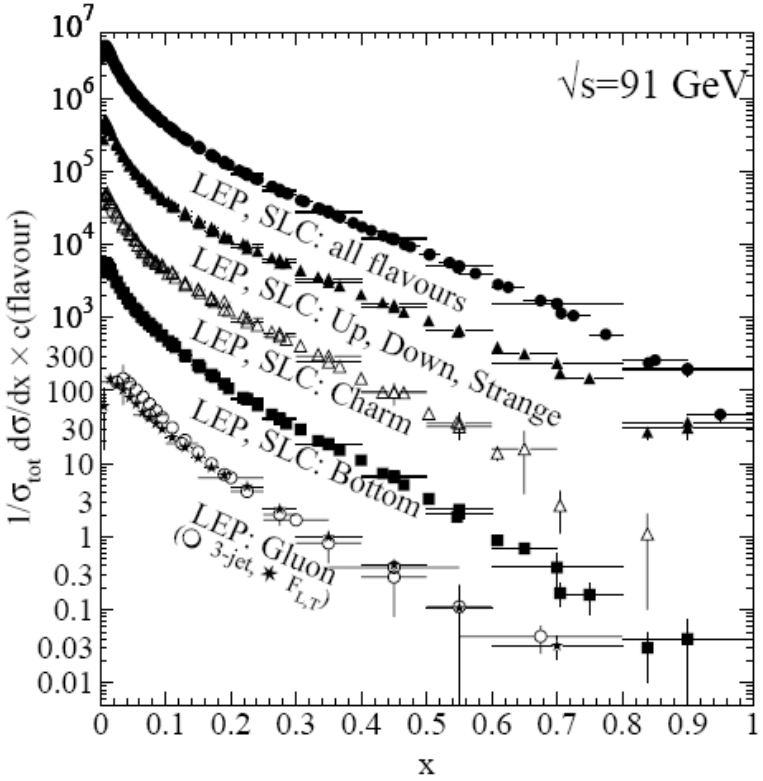

Figure 17.6: Comparison of the charged-particle and the flavour-dependent e^+e^- fragmentation functions obtained at $\sqrt{s} = 91$ GeV. The data [10,12,14,15,19,21] [22,28,59,61] are shown for the inclusive, light (up, down, strange) quarks, charm quark, bottom quark, and the gluon versus x. For the purpose of plotting, the distributions were scaled by $c(\text{flavour}) = 10^i$ where i is ranging from $i = 0$ (Gluon) to $i = 4$ (all flavours).

Fragmentation function (D- und B-Mesons)

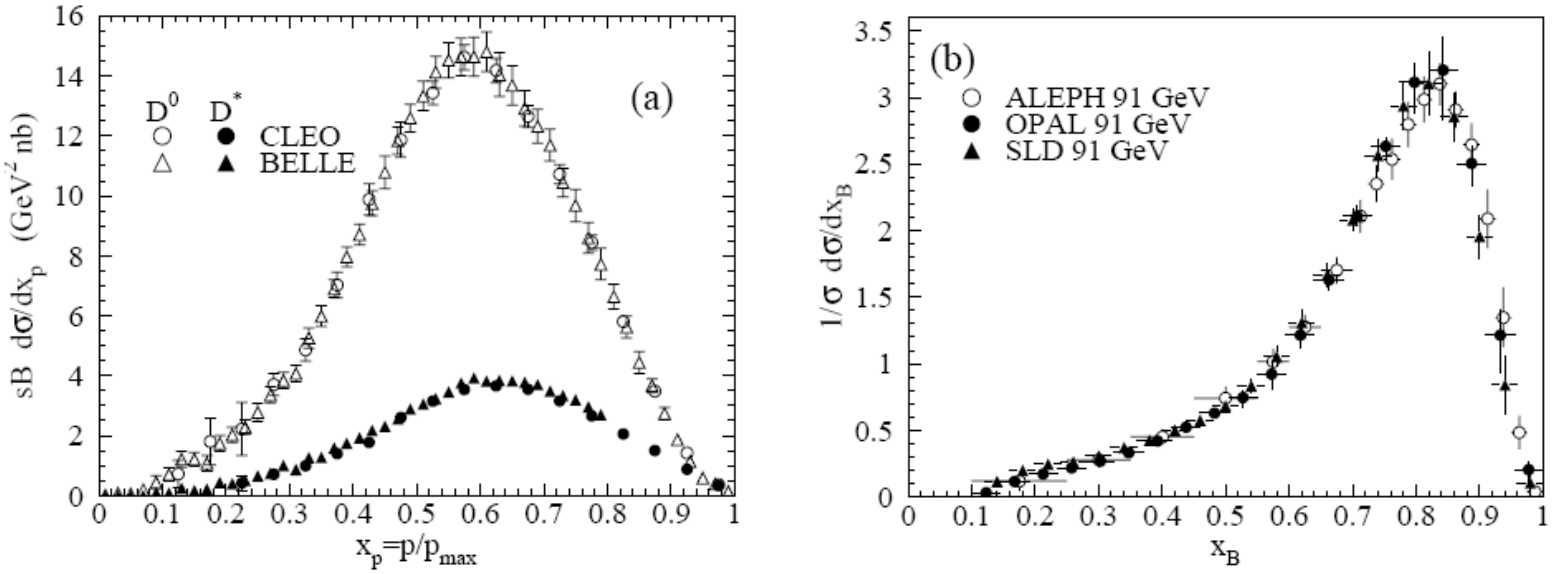

Figure 17.9: (a) Efficiency-corrected inclusive cross-section measurements for the production of D^0 and D^{*+} in e^+e^- measurements at $\sqrt{s} \approx 10.6$ GeV, excluding B decay products [121,122]. (b) Measured e^+e^- fragmentation function of b quarks into B hadrons at $\sqrt{s} \approx 91$ GeV [125].

2 and 3 jet events

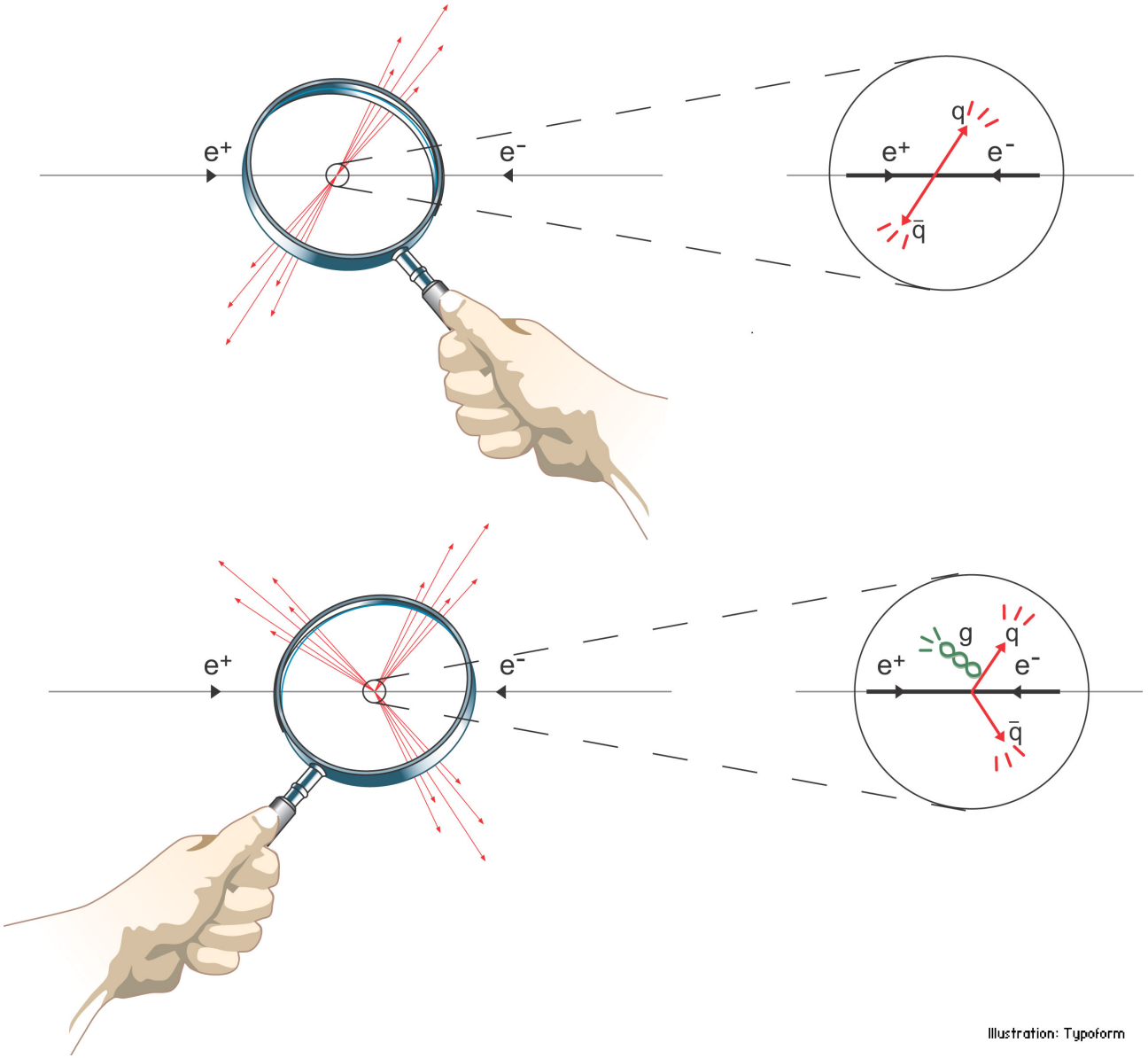

Jets in the Detector

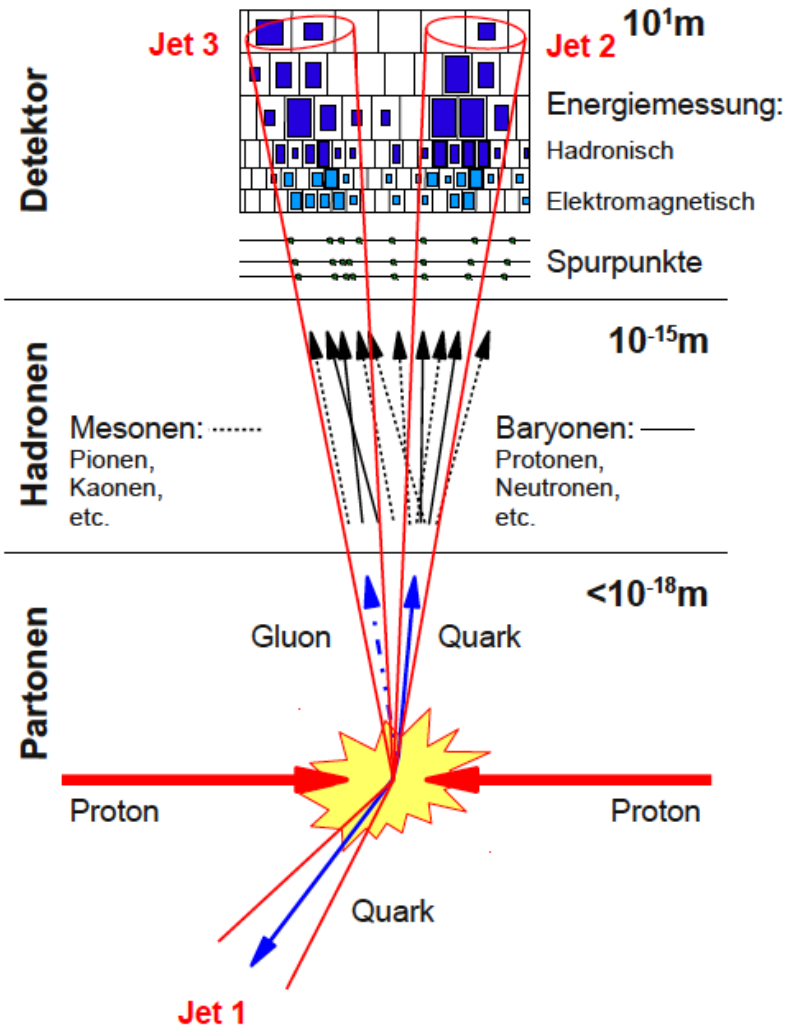

2-Jet Event in p+p bei $\sqrt{s}$ = 200GeV (STAR)

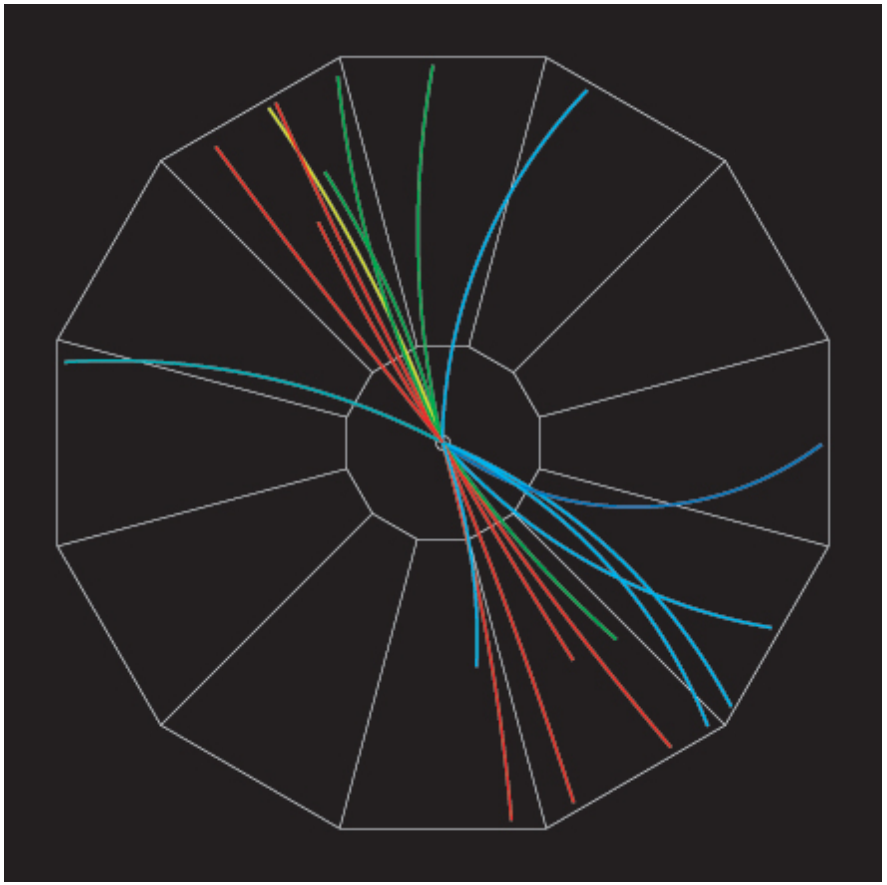

pQCD description of p_t-spectra

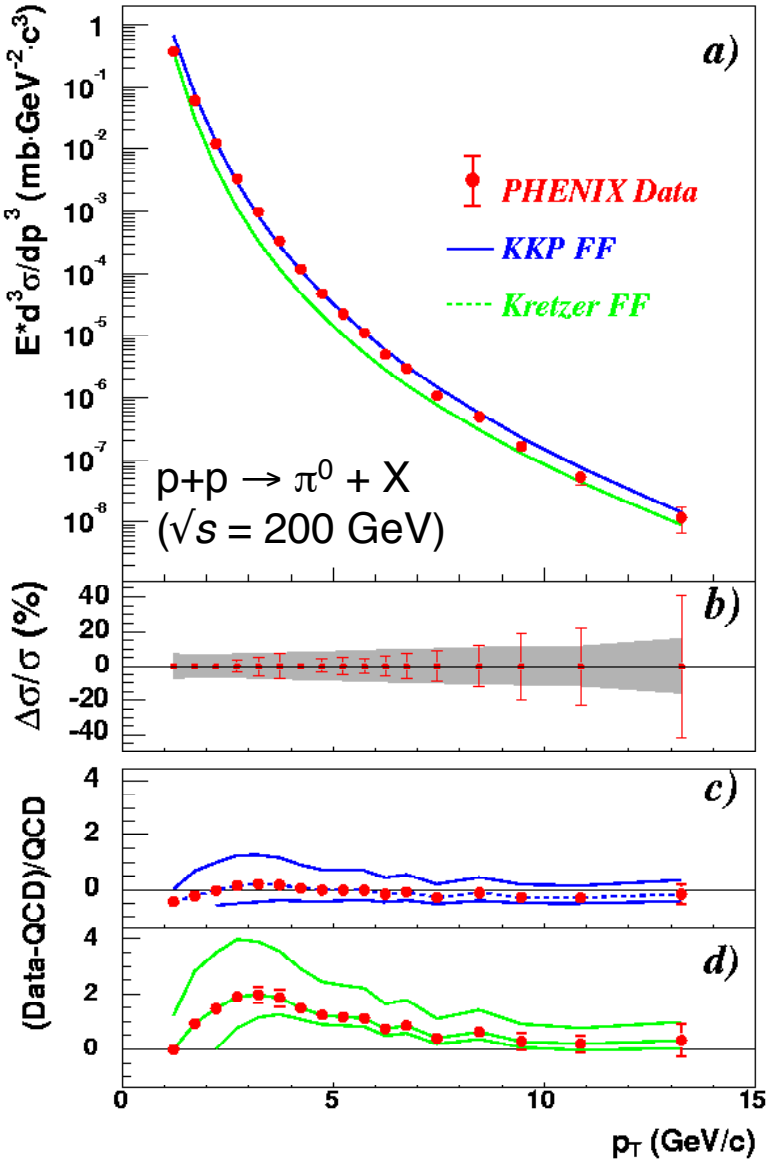

2-Jet event in p+p at √s = 7 TeV (CMS)

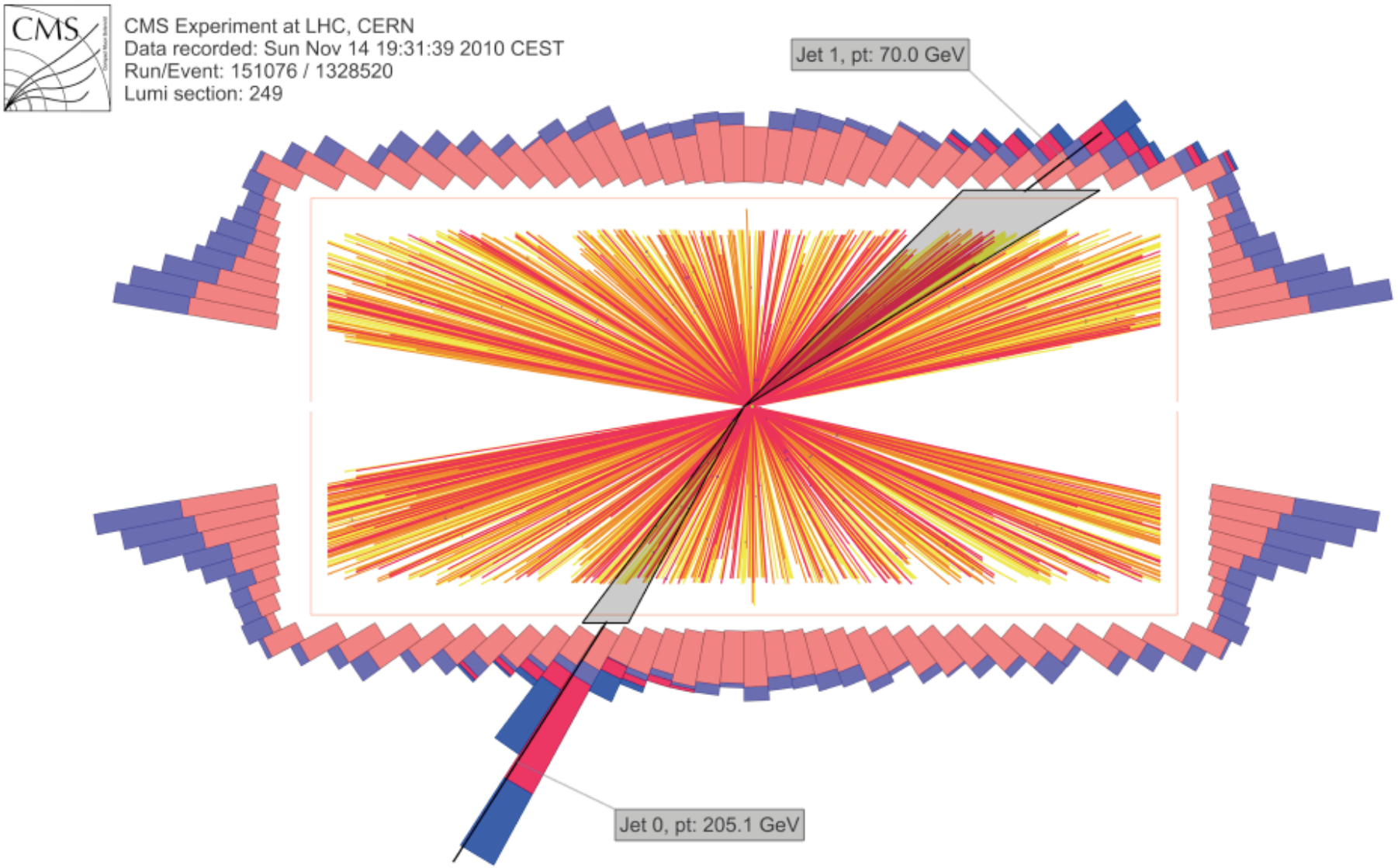

2-Jet Ereignis in p+p bei √s = 7 TeV (ATLAS)

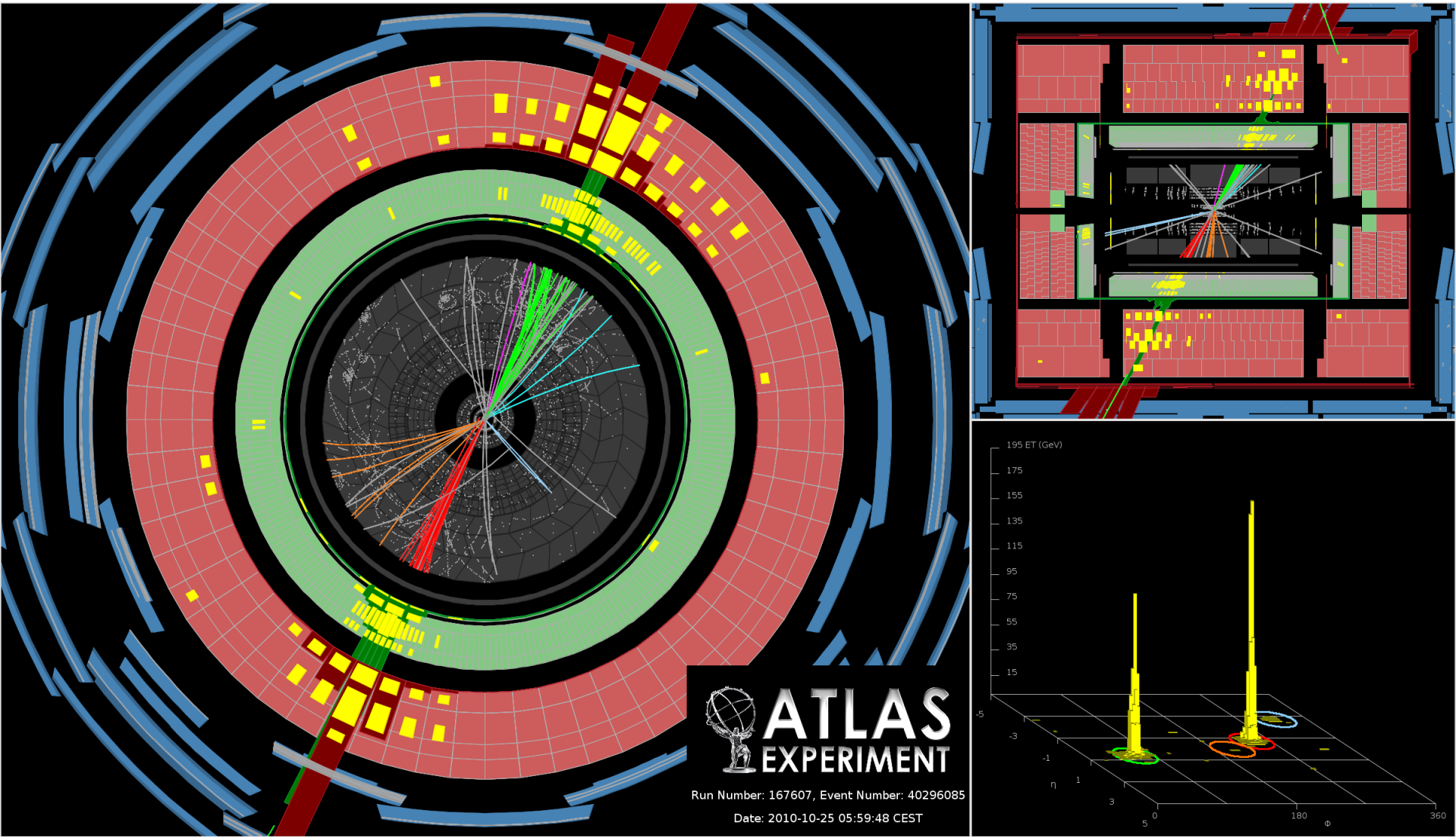

Jet finder

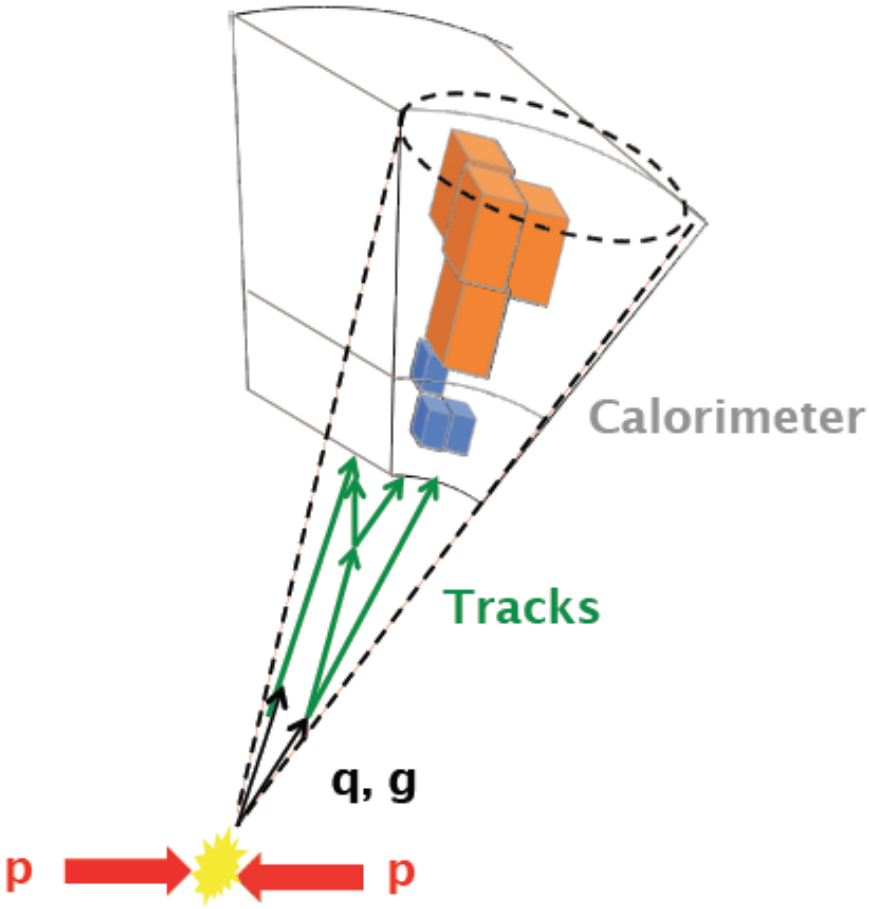

UA1 Cone Finder

Length = p_T

1)

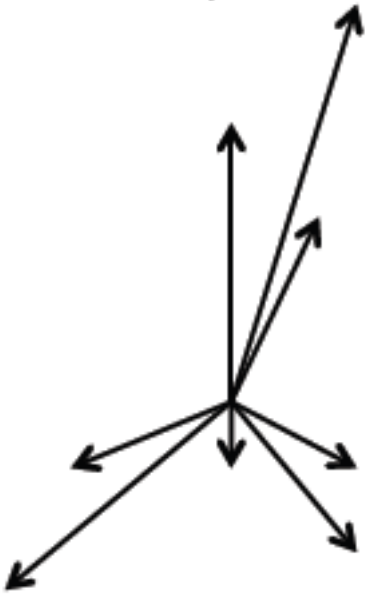

2)

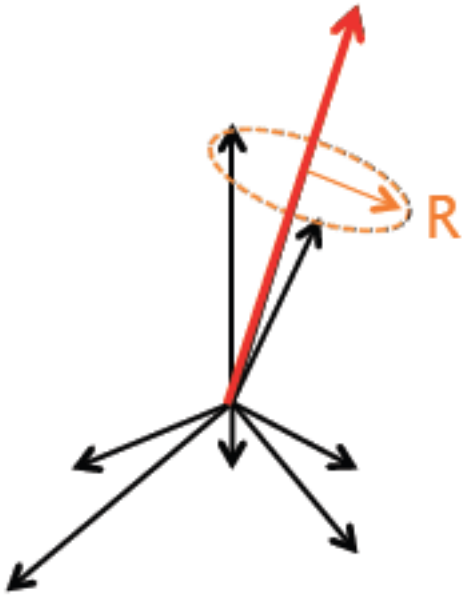

UA1 Cone Finder

3)

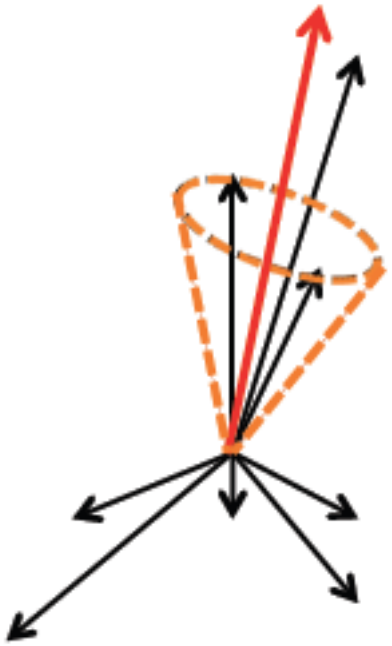

4)

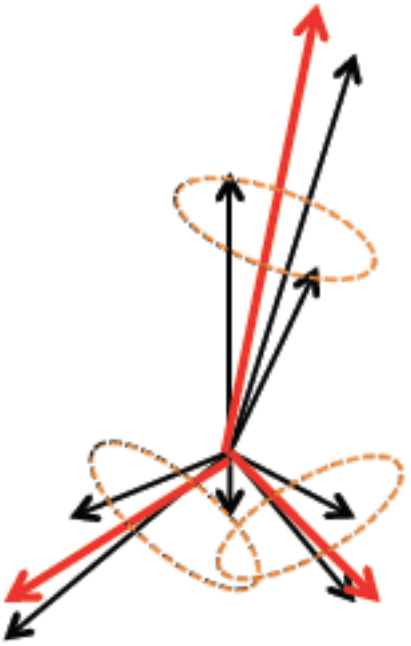

Cone-Radius

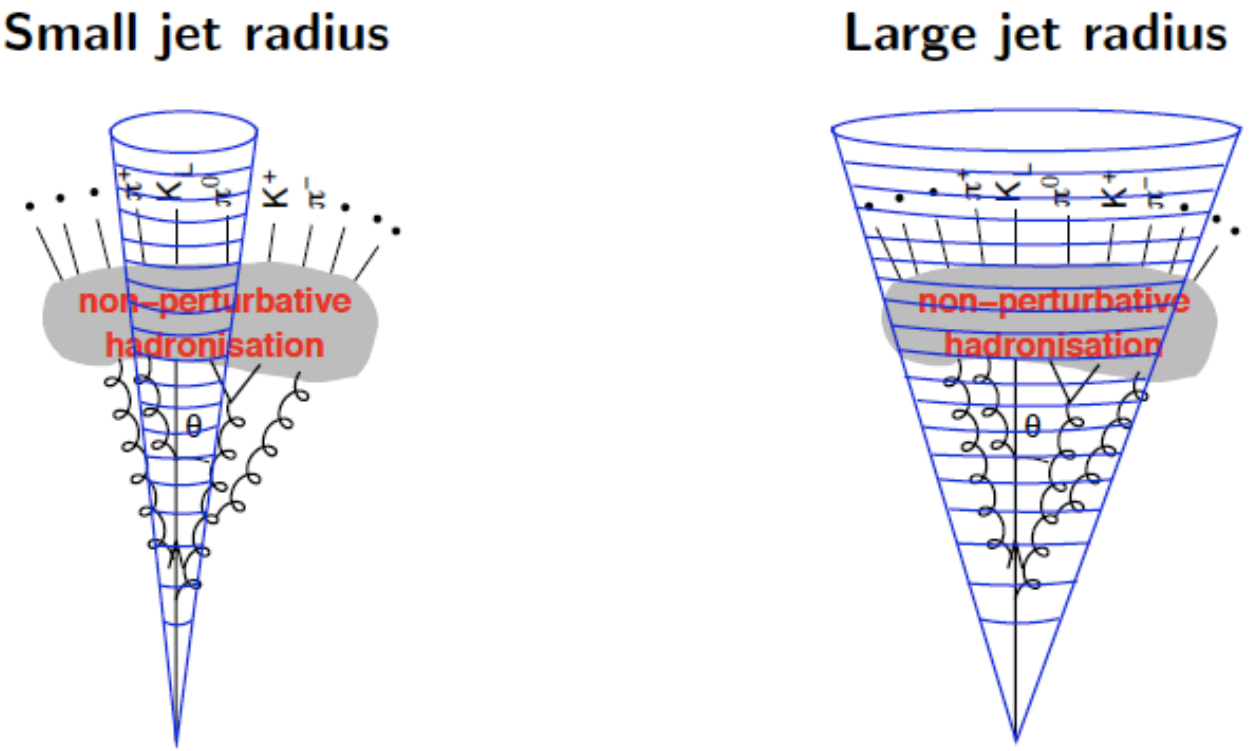
Small jet radius
non–perturbative
hadronisation
θ
Large jet radius
non–perturbative
hadronisation
θ

(Anti-)k_T Algorithmen

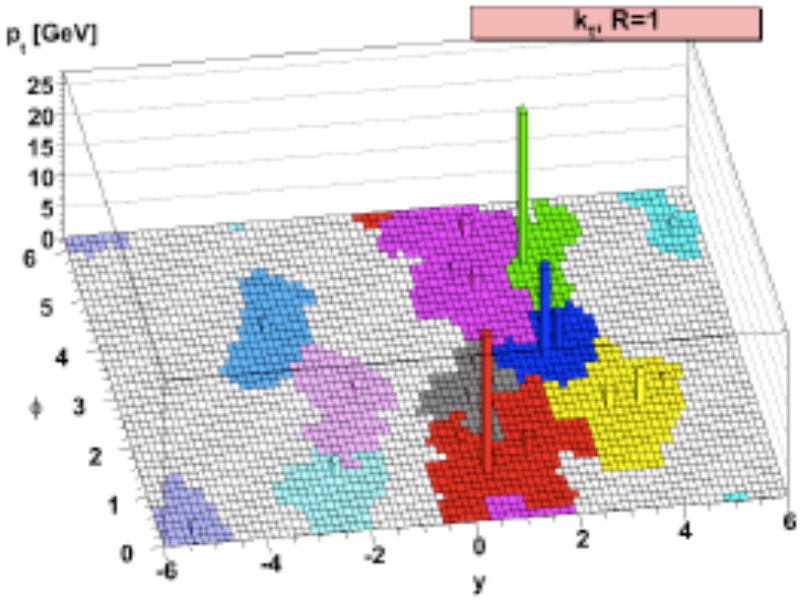

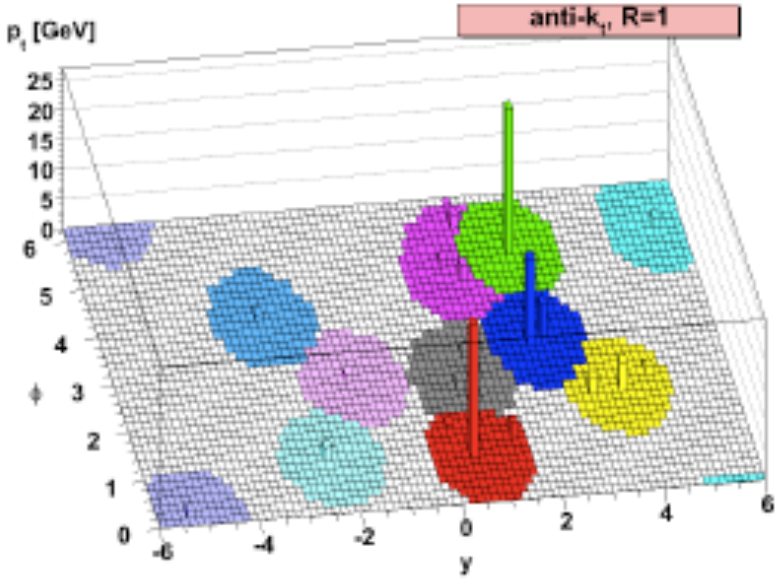

All particles are associated to jets

k_T: none circular shape

Anti-k_T: circular shape

High-p_t cross section from pQCD

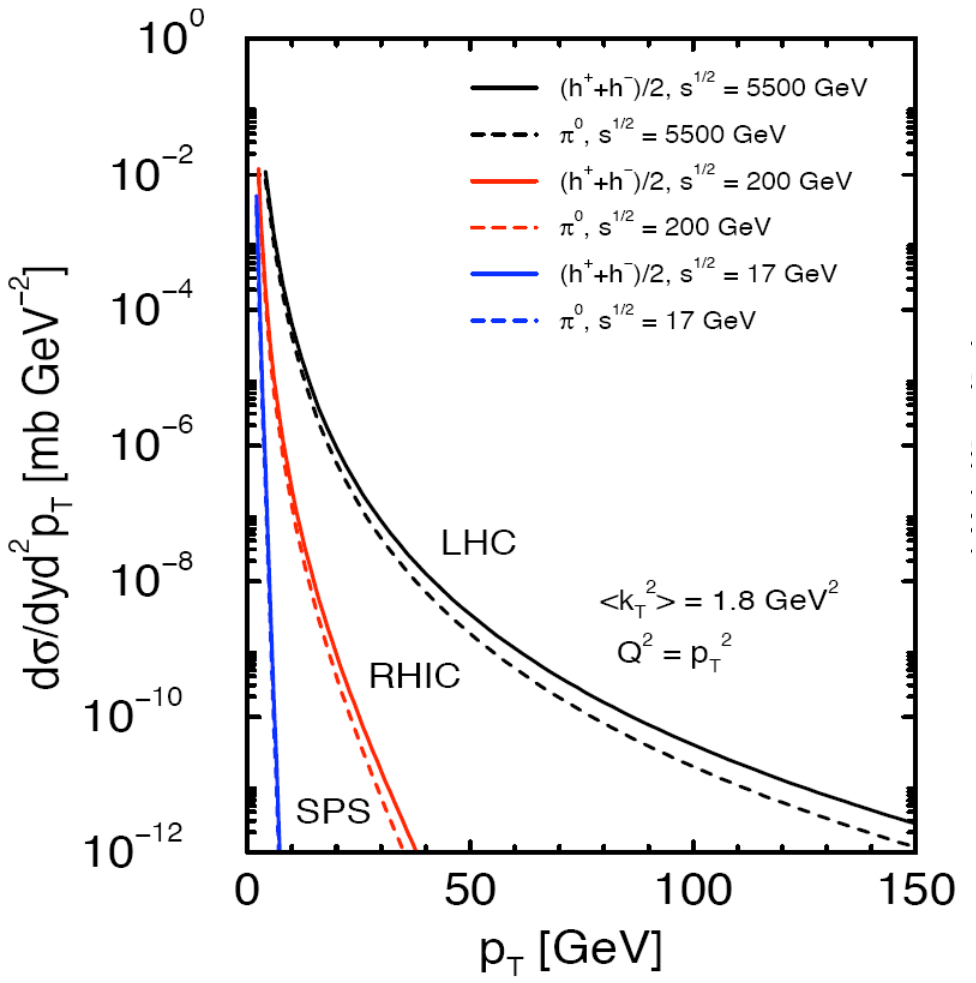

Contributions from parton processes

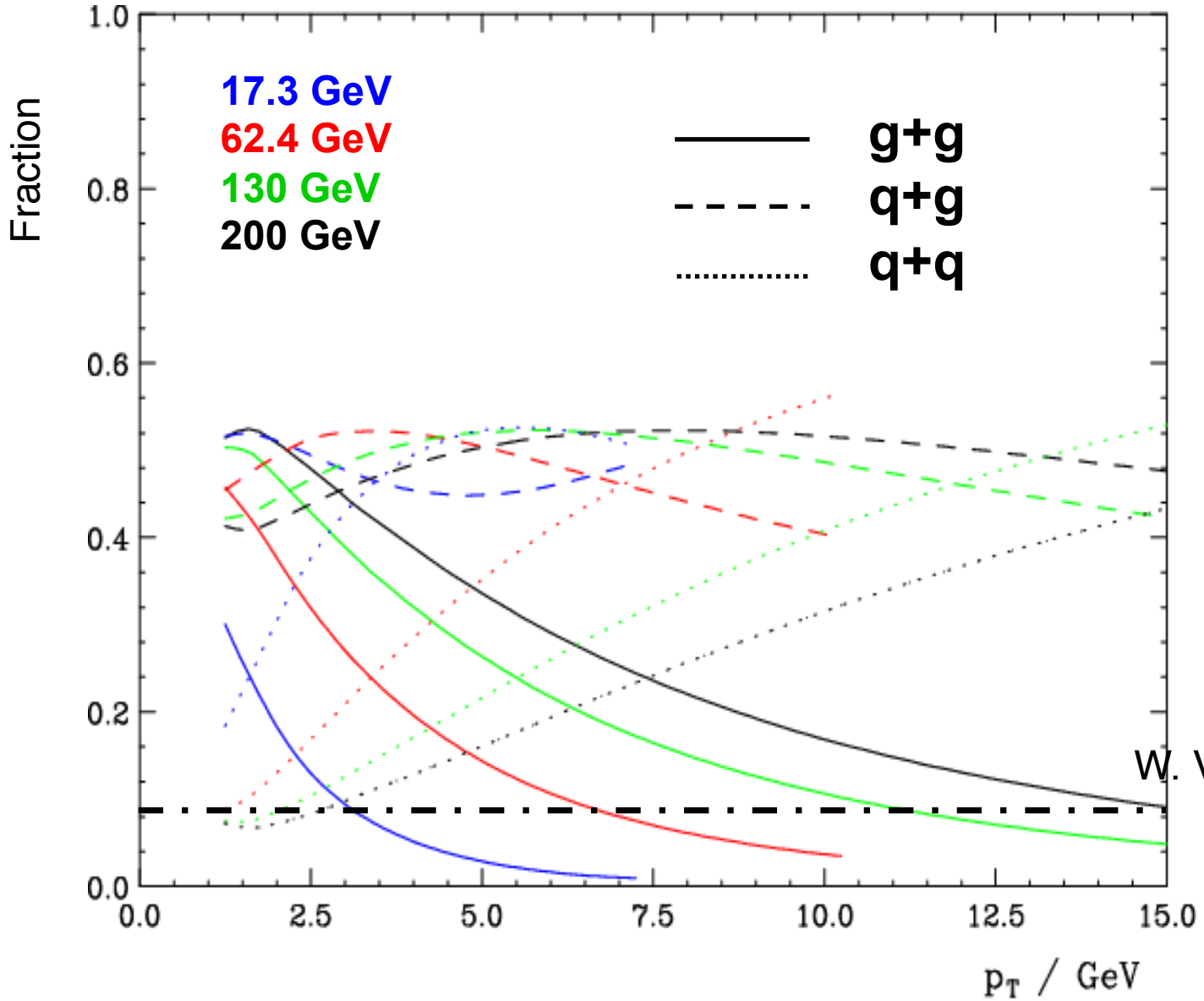

W. Vogelsang

Effect in p+A

Elastiic scattering of incoming partons
→ ,,k_t-broadening”

Energieloss of scattered partons
In cold nuclear matter

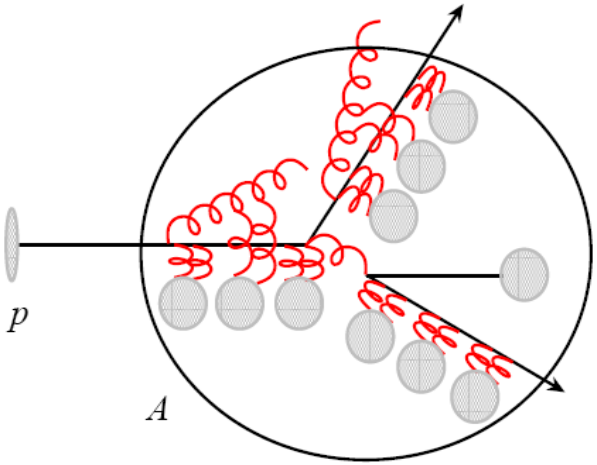

Jet Quenching

peripheral

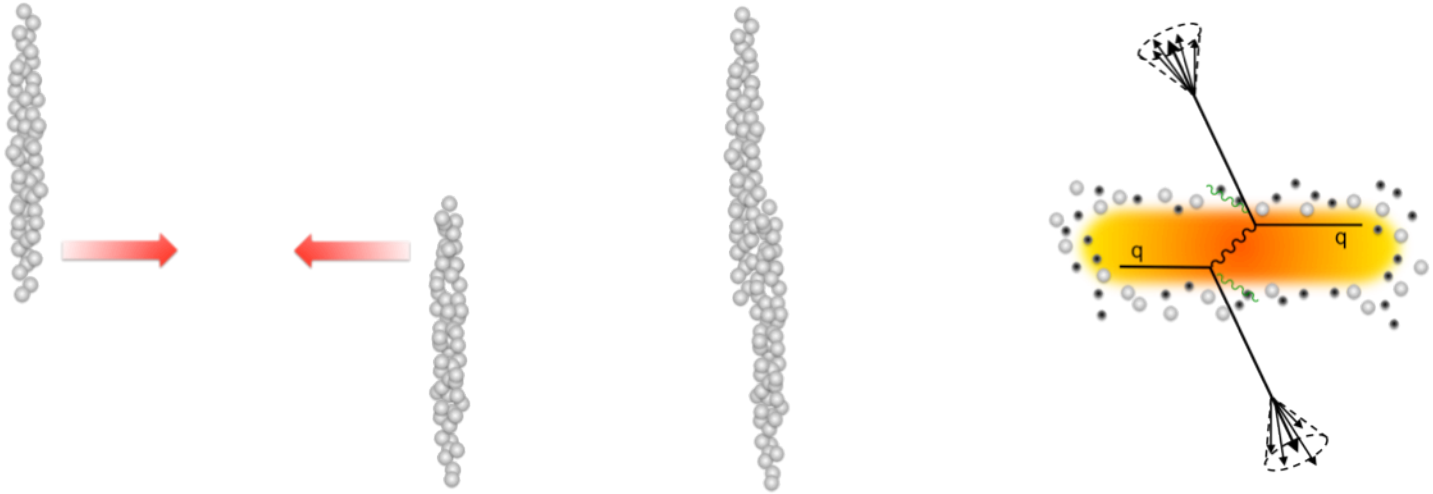

central

Energy loss of Partons

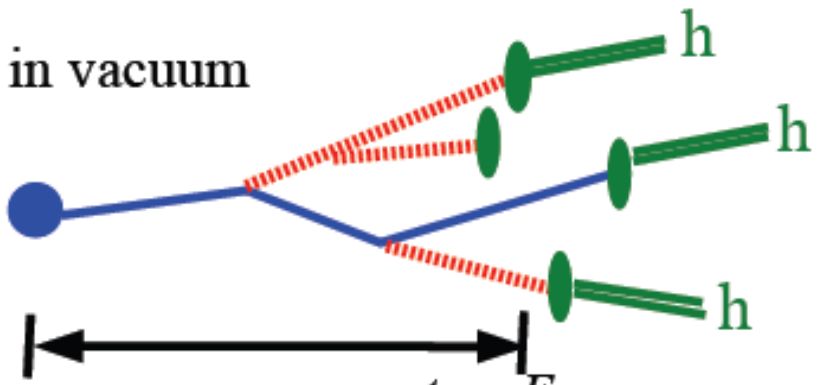

$$L_{hadr} \sim \frac{const}{Q_{hadr}} \frac{E}{Q_{hadr}}$$

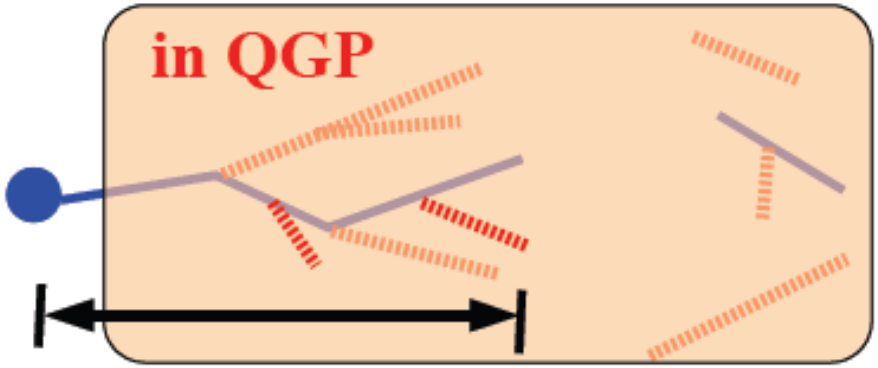

$$E \approx \Delta E = \frac{\alpha_s C_R}{4} \hat{q} L^2_{therm}$$

Nuclear Modification Factor R_{AA}

$$R_{AA}(p_t) = \frac{\sigma_{inel}^{pp}}{\langle N_{coll} \rangle} \frac{d^2 N_{AA}/(dp_t\, dy)}{d^2\sigma_{pp}/(dp_t\, dy)}$$

$$= \frac{1}{T_{AA}} \frac{d^2 N_{AA}/(dp_t\, dy)}{d^2\sigma_{pp}/(dp_t\, dy)}$$

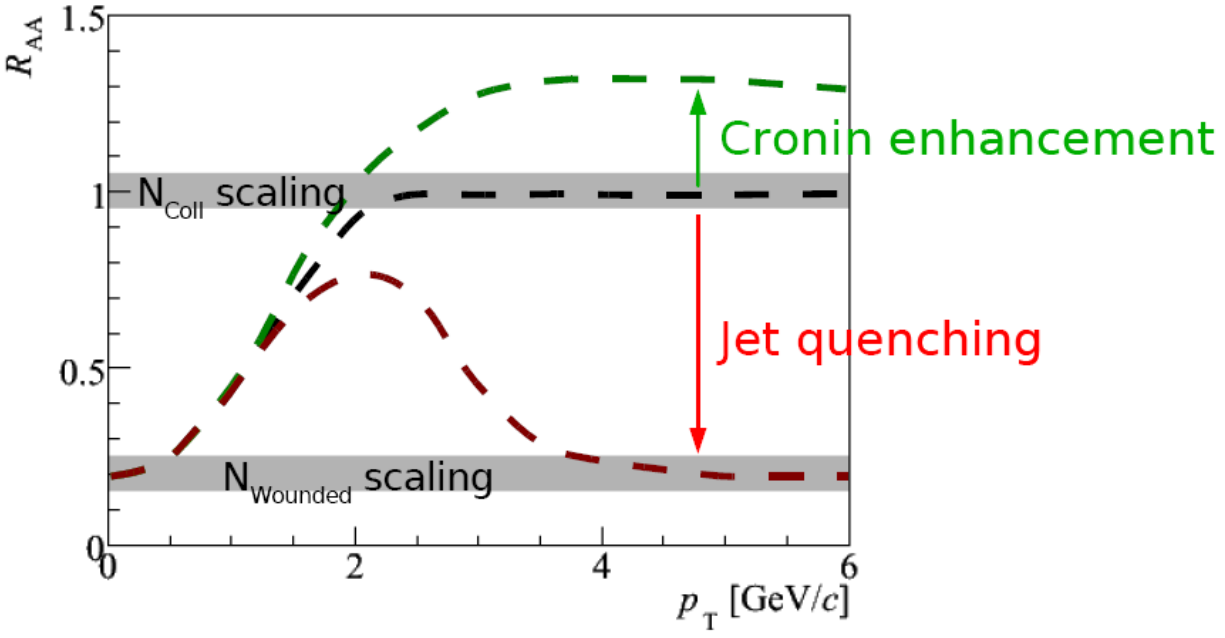

Nuclear Modification Factor (RHIC)

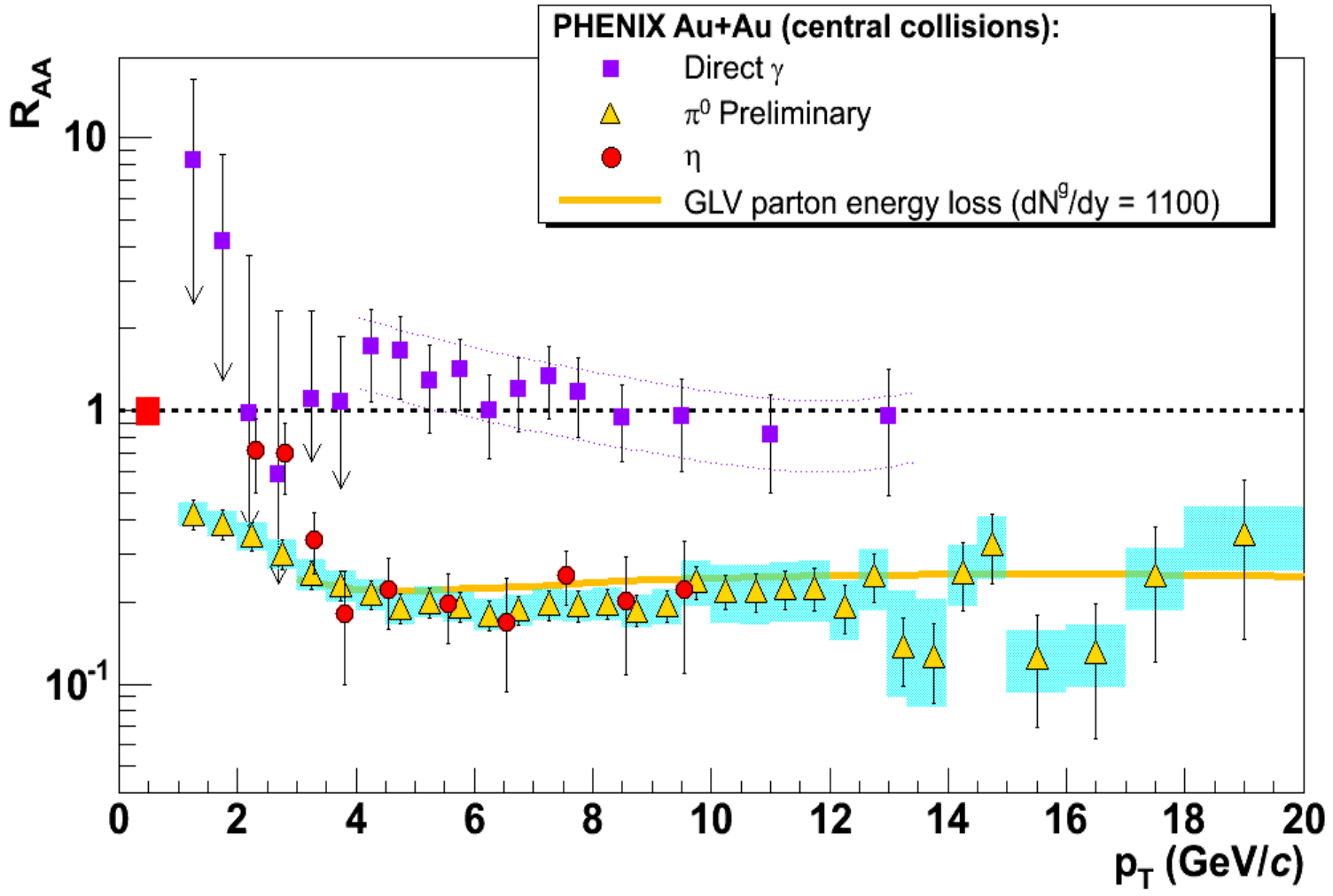

RHIC: Au+Au and d+Au Data

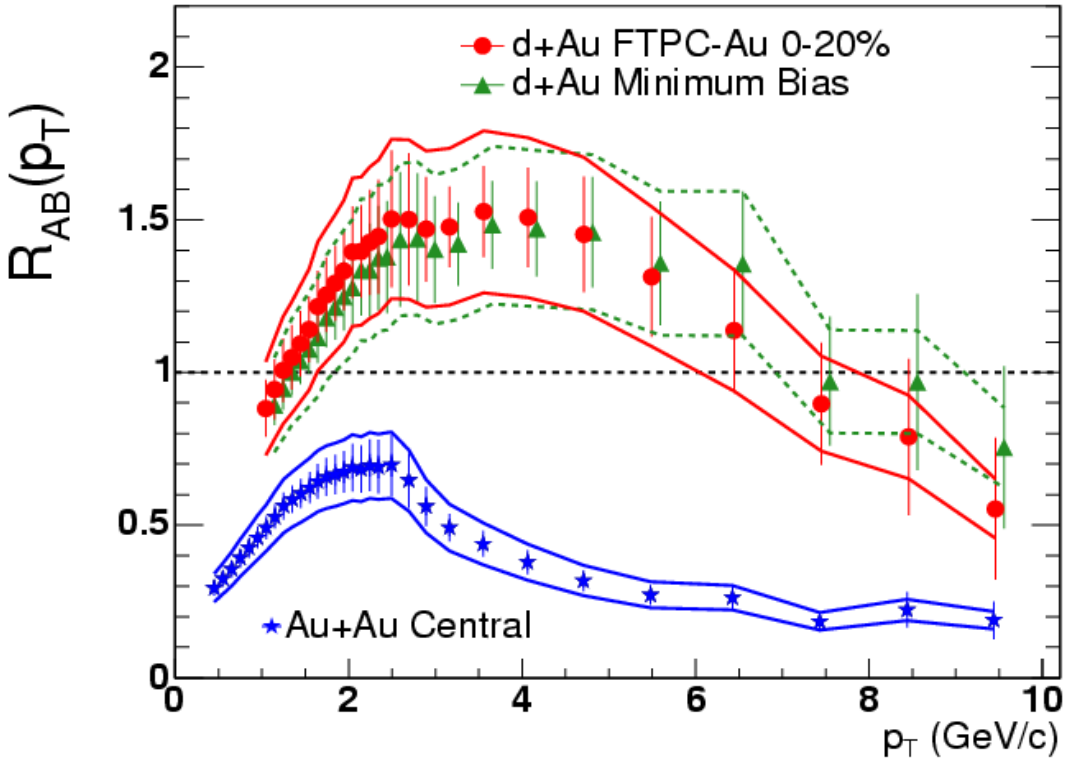

Nuclear Modification Factor (LHC)

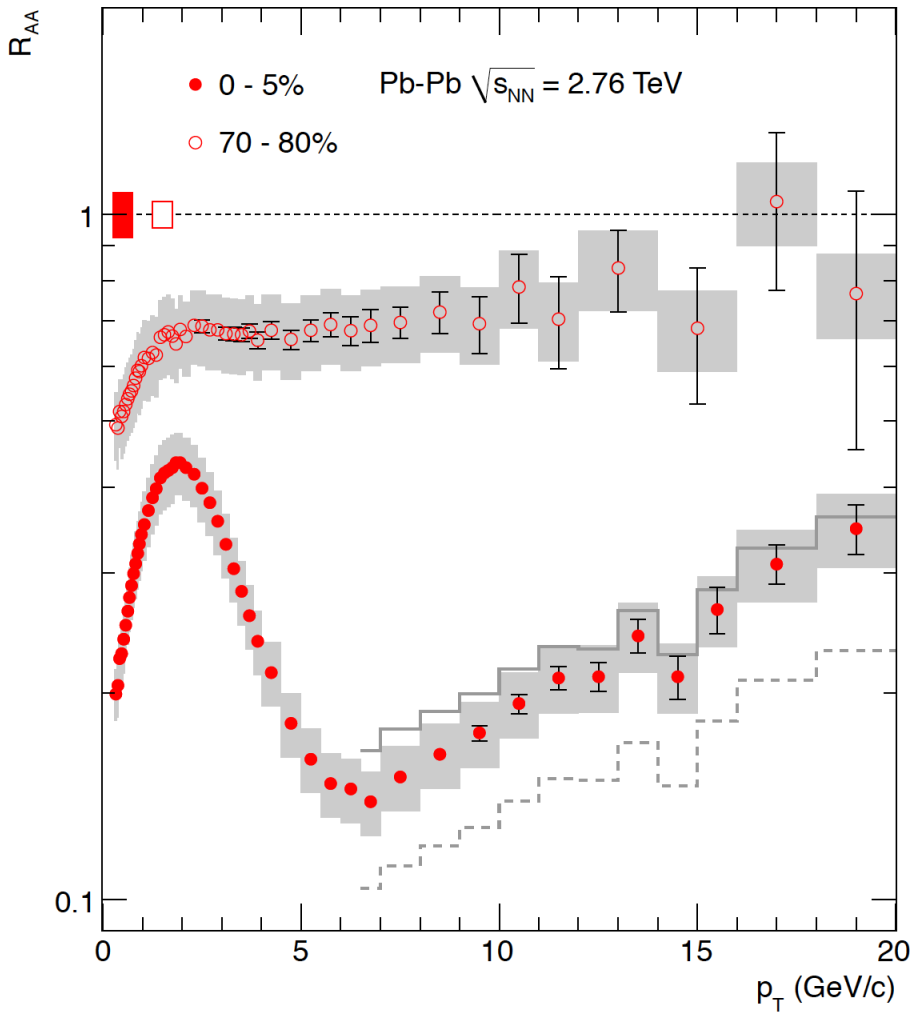

Nuclear Modification Factor (LHC and RHIC)

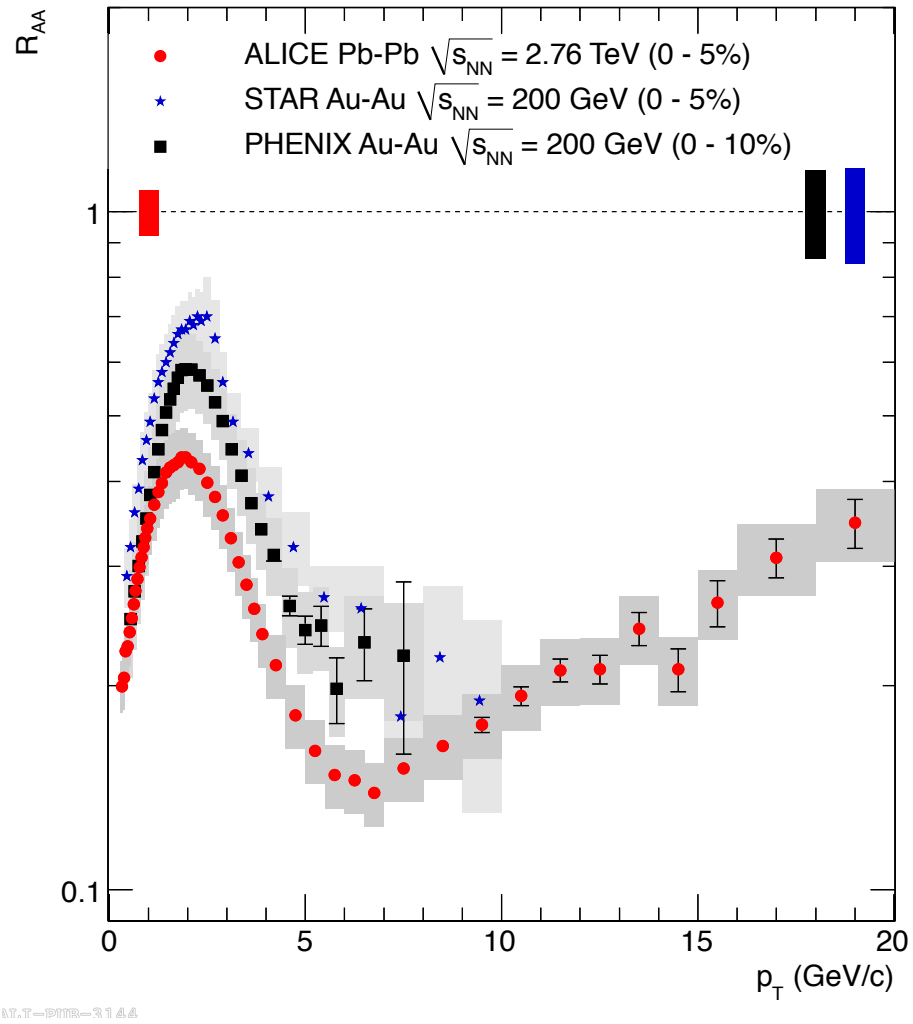

Azimuthal-Correlation

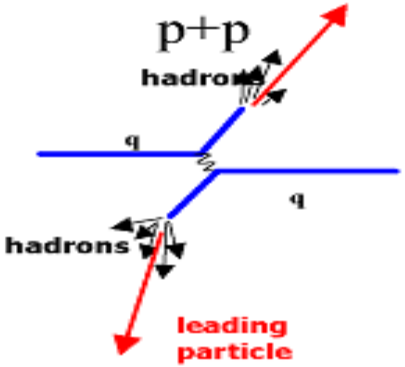

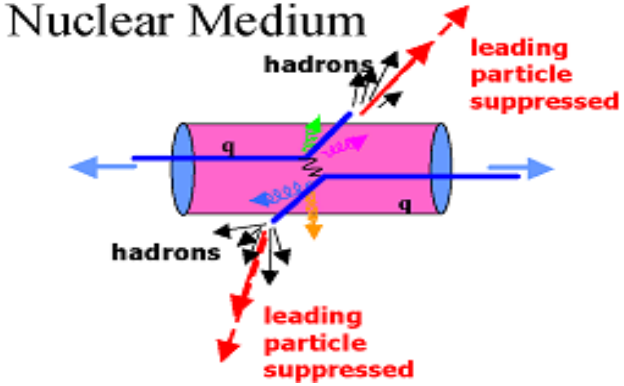

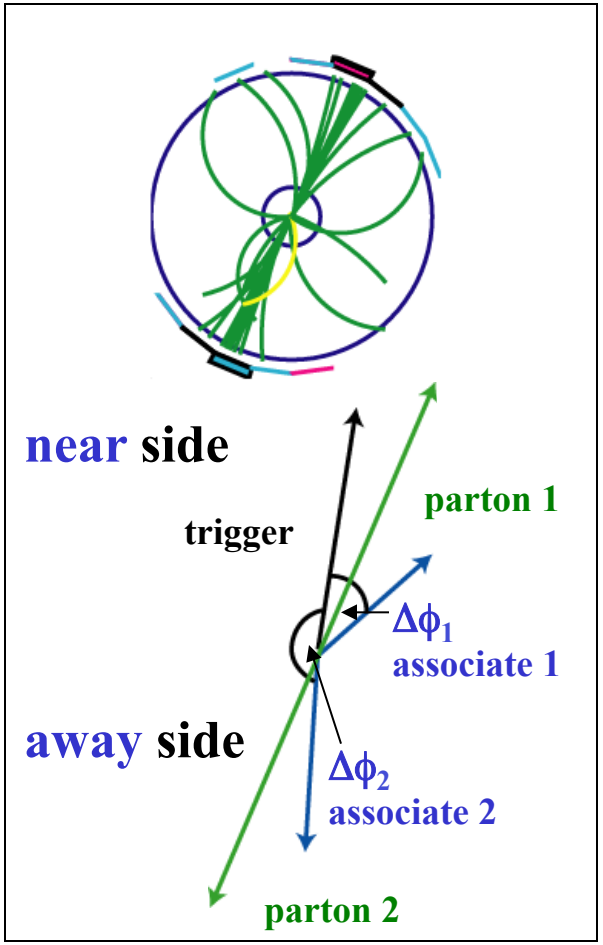

Azimuthal-Correlation: RHIC Data

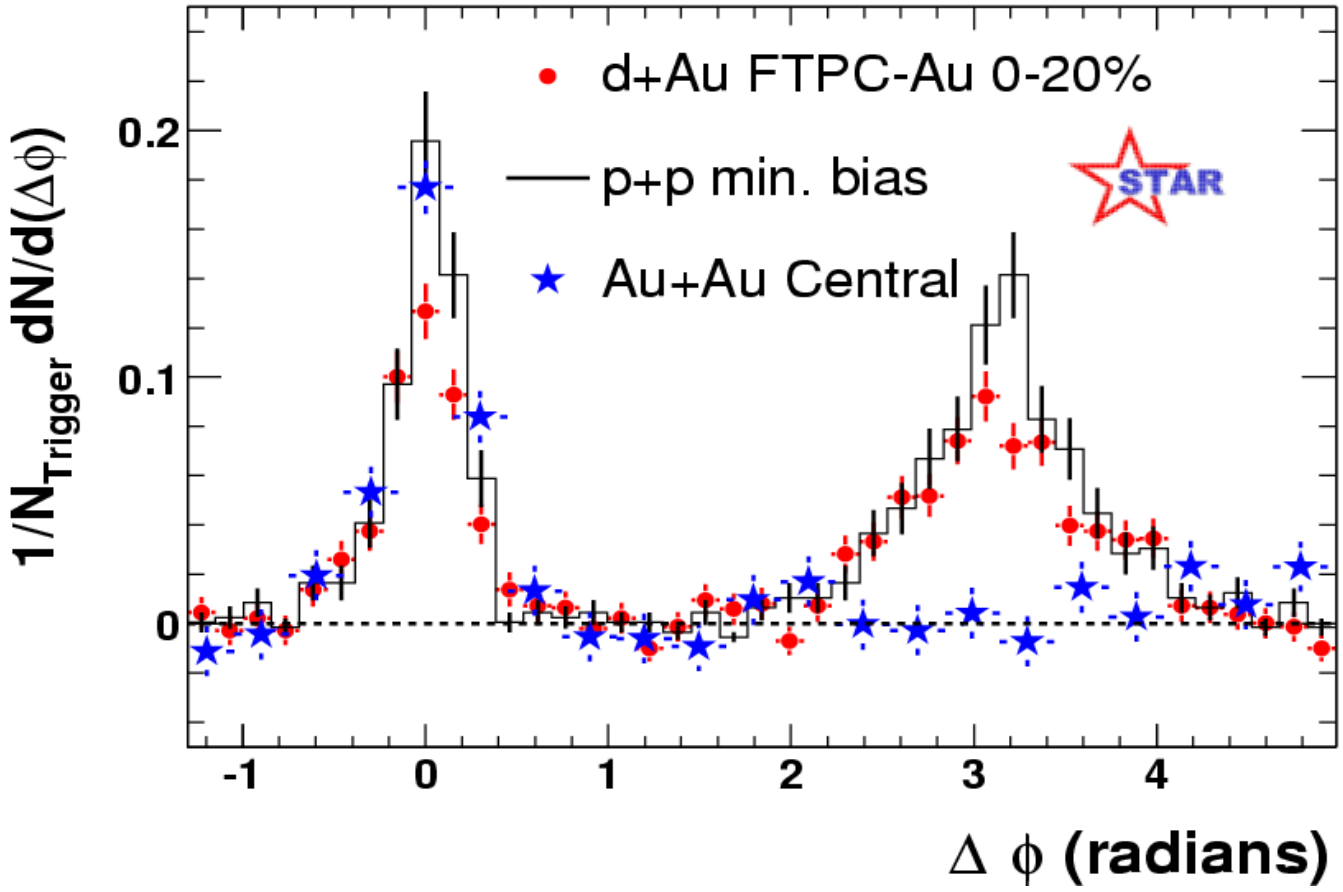

Trigger particle : 4.0 – 6.0 GeV/c
Associated particle: 2.0 – 4.0 GeV/c

$\Delta\phi\Delta\eta$ Correlation

d+Au

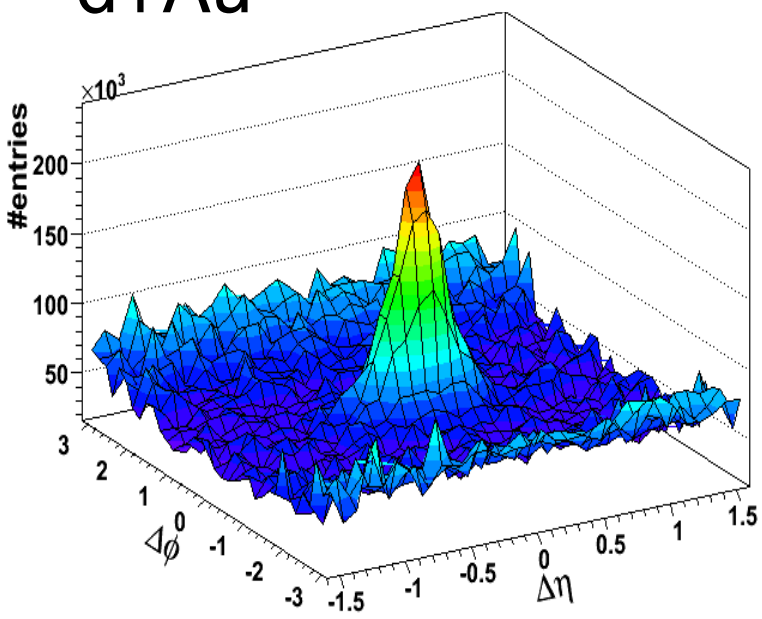

Au+Au

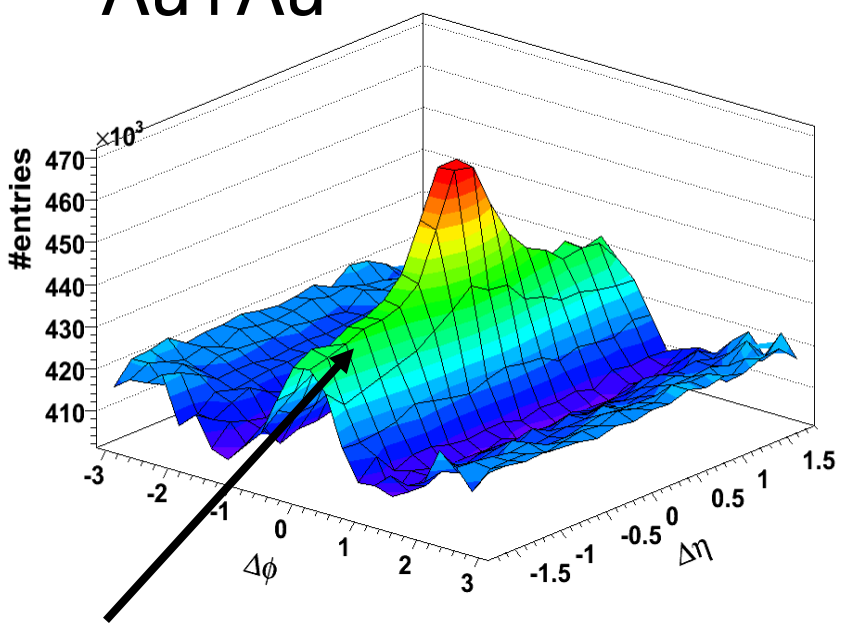

,,ridge”

Di-Jet Suppression at the LHC (CMS)

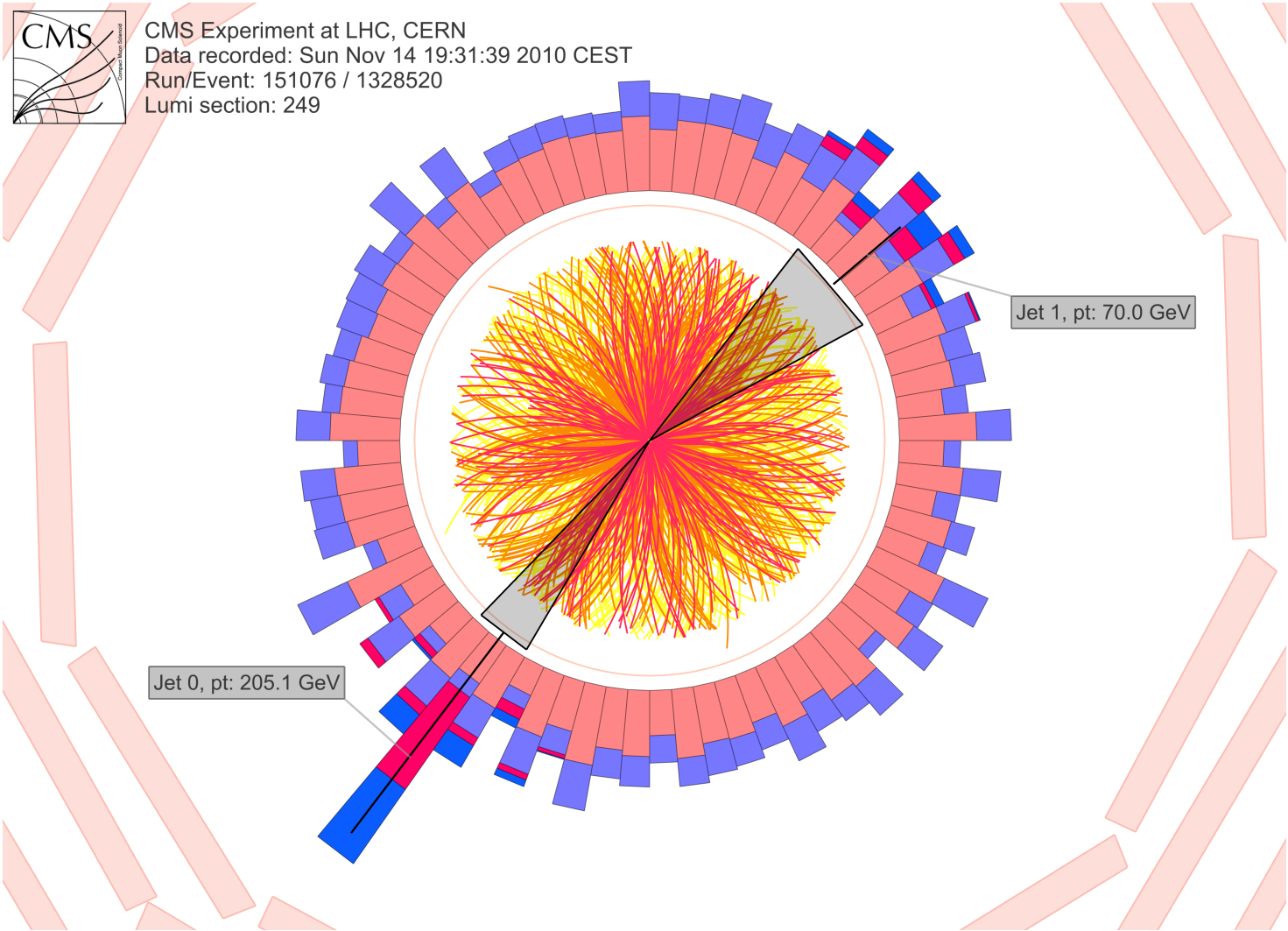

Di-Jet Unterdrückung am LHC (CMS)

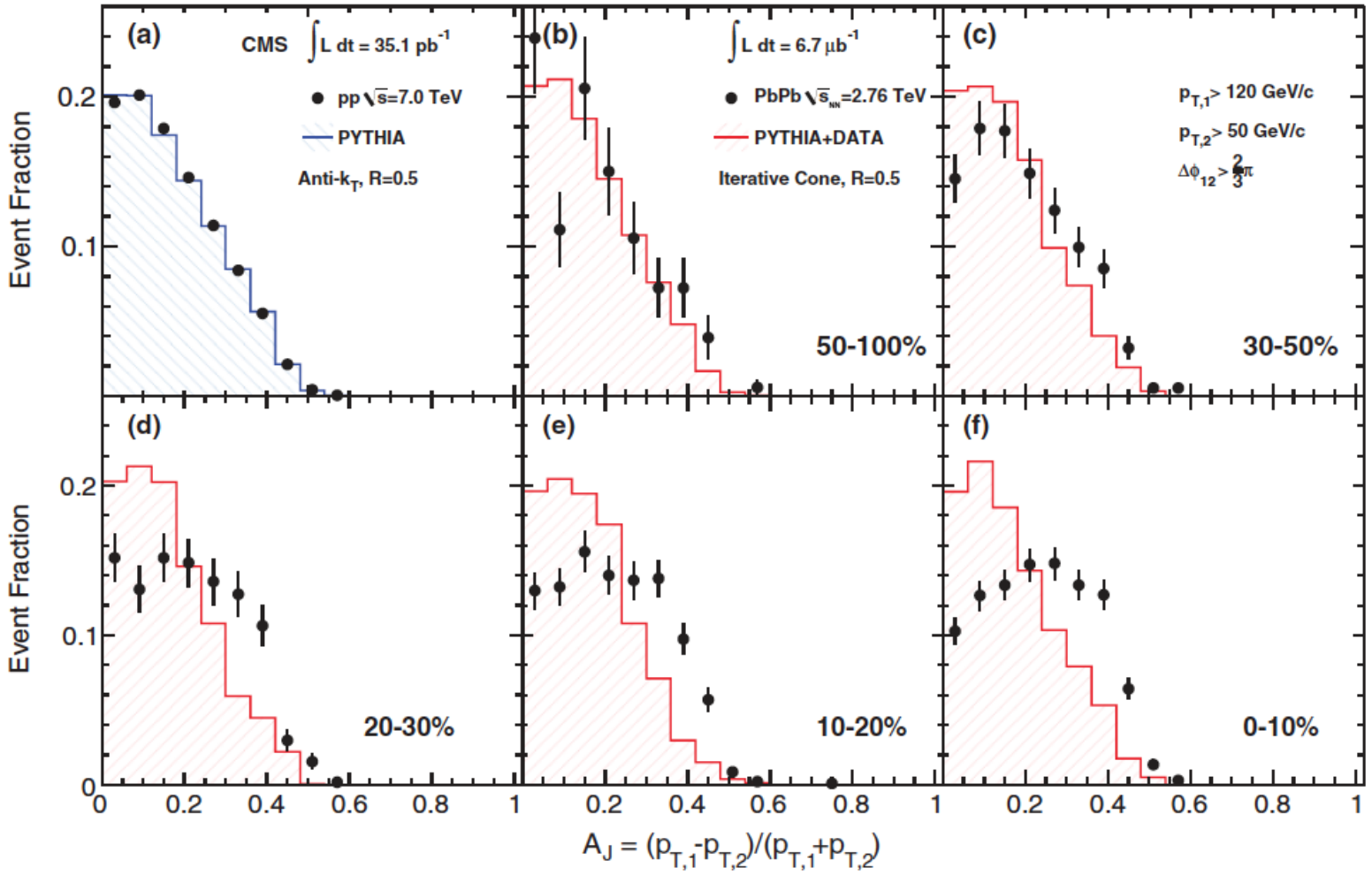

Jet-Suppression am LHC

$$R_{\mathrm{CP}}^{\mathrm{meas}}(p_{\mathrm{T}})|_{\mathrm{cent}} = \frac{1}{R_{\mathrm{coll}}^{\mathrm{cent}}} \left(\frac{\frac{N_{\mathrm{jet}}^{\mathrm{cent}}(p_{\mathrm{T}})}{N_{\mathrm{evt}}^{\mathrm{cent}}}}{\frac{N_{\mathrm{jet}}^{60-80}(p_{\mathrm{T}})}{N_{\mathrm{evt}}^{60-80}}} \right)$$

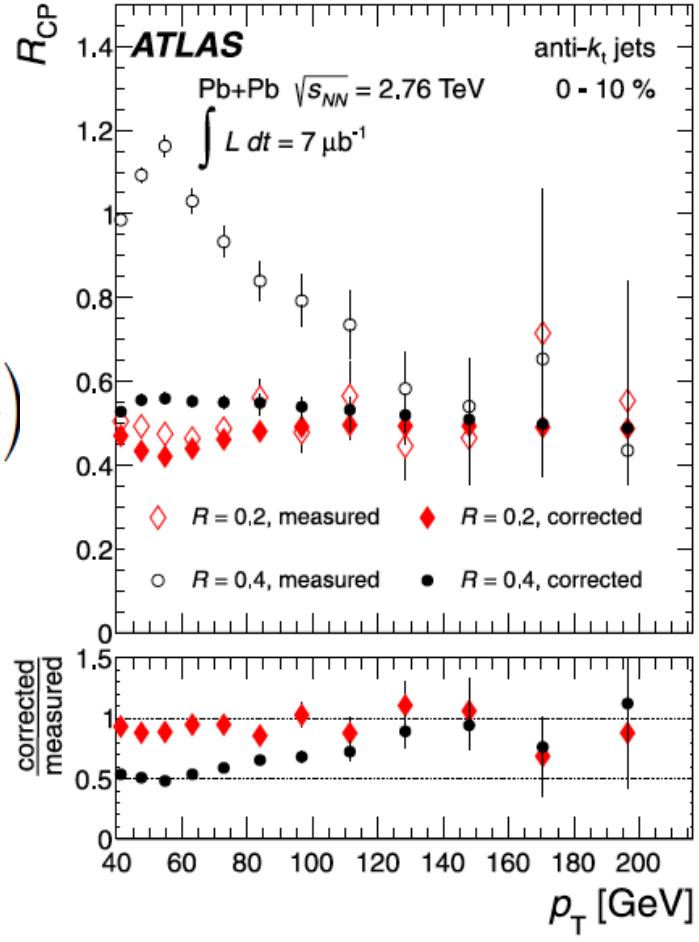

Fig. 3. Top: Measured and corrected R_{CP} values for the 0–10% centrality bin as a function of jet p_{T} for $R = 0.4$ and $R = 0.2$ jets. Bottom: Ratio of corrected to measured R_{CP} values for both jet radii. The error bars on the points represent statistical uncertainties only.

Jet-Suppression am LHC

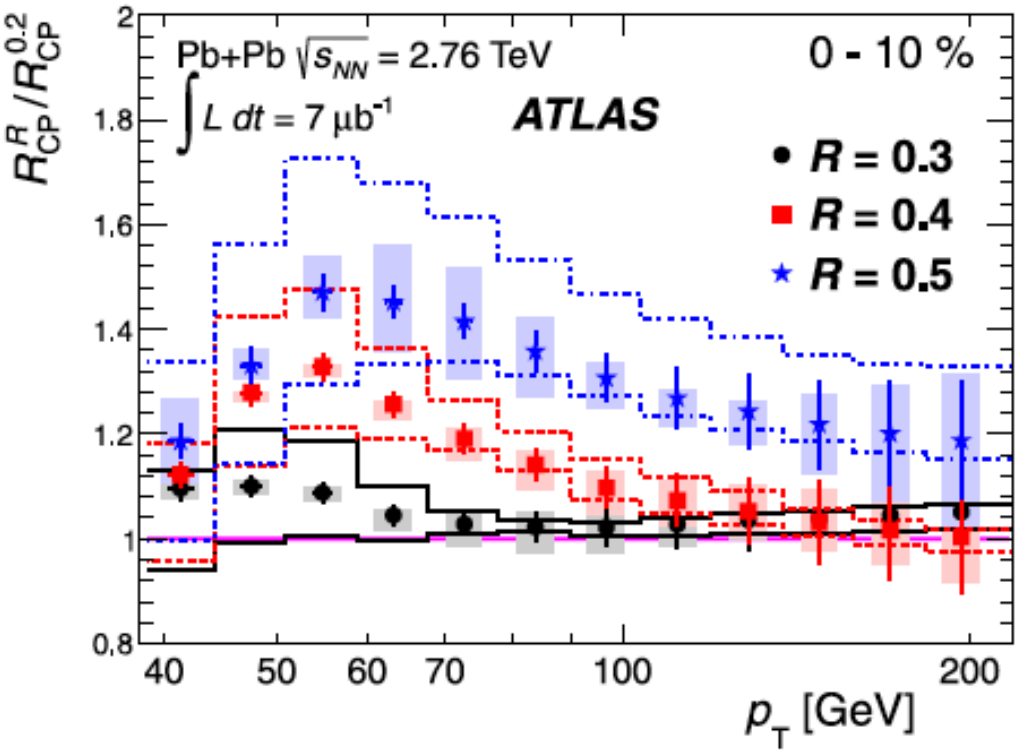

Fig. 8. Ratios of R_{CP} values between $R = 0.3, 0.4$ and 0.5 jets and $R = 0.2$ jets as a function of p_T in the 0–10% centrality bin. The error bars show statistical uncertainties (see text). The shaded boxes indicate partially correlated systematic errors. The lines indicate systematic errors that are fully correlated between different p_T bins.